

Wavelength Selection in Unstable Homoepitaxial Step Flow Growth

T. Maroutian, L. Douillard, and H.-J. Ernst

CEA Saclay, DSM/Drecom/Srsim, 91191 Gif-sur-Yvette, France

(Received 31 March 1999)

The growth of Cu on a vicinal Cu surface is investigated using variable temperature scanning tunneling microscopy. A meandering instability caused by the step edge barrier for diffusion leads to a lateral patterning of the surface with a temperature-dependent, distinctive wavelength. This length scale is set by nucleation of one-dimensional islands at step edges. In the temperature range covered by our experiment (230 to 400 K) a specific slope of the growth features within the plane of the surface is selected. This may point to a pronounced spatial anisotropy of the step edge barrier.

PACS numbers: 68.55.-a, 68.35.Ct, 81.15.Hi

Molecular beam epitaxy (MBE) and its analogs offer the possibility to fabricate solid state materials and artificial superlattices, structures with built-in periodicities at nearly any desired scale along the growth direction. A lateral structuring of materials with additional in-plane periodicities is the natural next step towards a functional modification of physical properties in a controlled manner. In general, current lithography schemes and other patterning techniques do not have sufficient spatial resolution to reach in-plane geometries at the nanometerscale, where, for example, quantum phenomena are expected to take place even at room temperature [1]. The use of inherent instabilities [2] in growth processes is currently being explored as a promising pathway for lateral nanostructuring. Such instabilities may be purely kinetic in origin (as evidenced on the basis of investigations of growth processes in homoepitaxial systems), associated with a larger energy barrier [the Ehrlich-Schwoebel (ES) barrier [3]] for diffusion of adatoms at and in the vicinity of steps with respect to diffusion on terraces.

On vicinal surfaces, which ideally are made up of terraces separated by regularly spaced steps of monoatomic height, growth proceeds not by nucleation of deposited atoms on terraces, but through incorporation on preexisting steps, which thereby advance. The ES barrier gives rise to an asymmetry in the adatom attachment to step edges favoring attachment from the lower side. While playing a stabilizing role during growth in the step train direction (TD) [3], the ES effect may induce a morphological instability along the step edge (step direction, SD), resulting in a transverse in-phase meandering of steps with a characteristic wavelength [4], which introduces thus an additional in-plane periodicity along SD. Since the pioneering work by Bales and Zangwill [4], numerous theoretical investigations have been devoted to this topic using continuum approaches [5,6] and Monte Carlo simulations [7]. Experimentally, very few studies address the predicted Bales-Zangwill (BZ) instability [8,9] and, in particular, no information on the meandering characteristics and its controlling parameters is available so far.

In this Letter, we report our study of homoepitaxial step flow growth on Cu (1,1,17) using variable temperature

scanning tunneling microscopy (VT-STM). We observe a collective, in-phase meandering of the steps with a wavelength selection along the SD. Wavelength and width of the step meander are reported for step flow growth at various substrate temperatures.

The experiments were performed with an Omicron VT-STM. The base pressure in the ultrahigh vacuum chamber was 2×10^{-10} mbar. The Cu (1,1,17) sample had been desulfurized by heating at 1170 K under H_2 flow for 2 months. The surface was cleaned *in situ* by repeated cycles of 600 eV Ar ion sputtering and annealing to 650 K. After the last cycle, the sample was slowly cooled down to the desired deposition temperature, ranging from 230 to 400 K. During deposition, the sample temperature was controlled with ± 5 K. The desulfurized Cu source was located about 10 cm in front of the sample at normal incidence. The incident flux was calibrated with a quartz balance, and set to 3×10^{-3} monolayer (ML)/s in most experiments. After deposition of about 5 ML, the sample was transferred to the STM stage and quenched to below 180 K prior to imaging. During sample transfer, which took about 2 min, the temperature rise was less than 5 K. We have checked explicitly that under these conditions the meandering characteristics that have developed during step flow are preserved.

The Cu (1,1,17) surface is made up of (001) terraces separated by steps of monoatomic height parallel to the $[\bar{1}10]$ direction. The mean terrace width is $l = 21.7 \text{ \AA}$, and the nearest-neighbor distance $a = 2.55 \text{ \AA}$. Figure 1(a) shows a $310 \times 200 \text{ \AA}^2$ STM image of the surface prior to deposition [10]. One observes regularly spaced steps with straight edges parallel to the $[\bar{1}10]$ direction. Larger scans taken at different positions on the sample surface all displayed a similar topography, characteristic of a long-range ordered Cu (1,1,17) vicinal surface. Figure 1(b) is a $640 \times 640 \text{ \AA}^2$ representative image of the surface after step flow at $T = 245 \text{ K}$. In marked contrast to the straight edges observed prior to Cu deposition, the steps now exhibit a collective, in-phase large amplitude meandering, correlated both along the SD and perpendicularly to it. Distinctive patterns are seen, due to the phase adjustment in the TD. Along the SD, a characteristic length emerges,

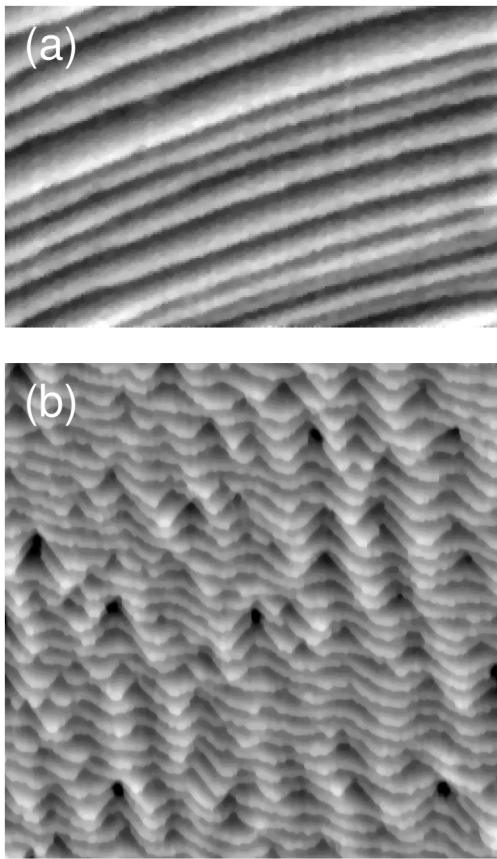


FIG. 1. STM topographs (high-pass filtered) of the Cu (1,1,17) vicinal surface recorded at 180 K. The mean terrace width is 21.7 Å. (a) $310 \times 200 \text{ \AA}^2$ image, prior to Cu deposition. Tip bias -2 V , tunneling current 0.9 nA . Note that step fluctuations are partially frozen in, because of kinetic limitations at that low temperature. (b) $640 \times 640 \text{ \AA}^2$ image after deposition of 5 ML Cu at a flux of $3 \times 10^{-3} \text{ ML/s}$ and a surface temperature of 245 K. Tip bias -1 V , tunneling current 0.3 nA . During step flow the whole step train is translated 5 terrace widths relative to its position prior to deposition. A transverse, in-phase meandering of steps is observed, leading to the formation of characteristic growth patterns, or "fingers."

corresponding to the distance between these patterns, or "fingers," which form where the meandering has a well-defined wavelength together with a phase adjustment over several steps. Between such regions the step edges are weakly modulated. In regions of large amplitude meandering, angular points (the darker regions) are formed on the step edge and a characteristic slope is selected at each side of the fingers. These local orientations of the step edge are found to be close to the $\langle 100 \rangle$ direction. Experiments in which we have deposited 50 ML instead of 5 ML show that the phase correlation along TD improves with increasing coverage. This topography can be reverted to that of the pristine equilibrium structure simply by annealing the sample for a couple of hours to 650 K.

Similar morphologies develop as well during step flow for surface temperatures from 230 to 400 K. In order to determine the characteristic meandering wavelength and the step width for each temperature, 5 to 10 STM images

were taken at different positions on the sample. For each image, about 10 wavelength measurements were made, by picking up the distance between fingers. Step edge profiles $\zeta(x)$ were extracted to compute the step width from $w = \sqrt{\langle \zeta^2 \rangle}$. The wavelength and the step width are then taken as the average of each mean value on the images for a given temperature. Length calibration made use of the fact that the step flow growth is stable versus fluctuations along the TD [8]. The value of the mean terrace width on all images is thus equal to l . Note that local perturbations of the step profile caused by impurities acting as pinning centers were readily identified and excluded from the measurements.

The temperature dependence of both the wavelength λ and the step width w shows an Arrhenius-type behavior, as seen in Fig. 2. Expressed in units of l , λ ranges from 2 at $T = 230 \text{ K}$ to 10 at $T = 400 \text{ K}$, with a slope of $76 \pm 11 \text{ meV}$, and w from 0.2 to 1.2 at $T = 355 \text{ K}$ with a slope of $92 \pm 8 \text{ meV}$. Thus both λ and w increase with temperature, while keeping the ratio w/λ nearly constant. This surprising finding is corroborated by our observation that the selected orientation of the sides of the fingers is found always close to the $\langle 100 \rangle$ direction in the whole temperature range covered by our experiment. Preliminary experiments reveal that the same patterns are generated also during step flow in Cu (1,1,9), and that the wavelength increases with decreasing flux.

Inherently unstable homoepitaxial step flow growth leads thus to a patterning in the plane of the surface with specific meandering characteristics. Which parameters control the wavelength? Is this lateral nanostructuring the manifestation of the BZ instability? This instability can be traced back to different kinetics for the attachment of adatoms to ascending and descending steps, which has its origin in the ES barrier associated with descending steps [3]. Because of the higher probability for a diffusing

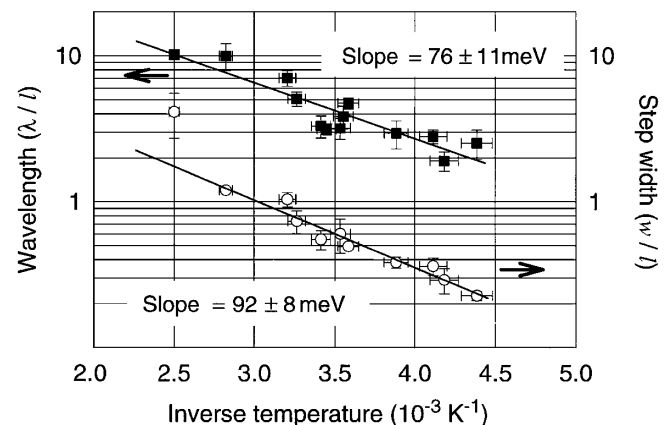


FIG. 2. Wavelength λ (■) and step width w (○), as determined from STM images after deposition of 5 ML Cu at a flux of $3 \times 10^{-3} \text{ ML/s}$, and plotted versus inverse deposition temperature. Both w and λ are expressed in units of the mean terrace width l . Straight lines are least-squares fits (excluding the point at 400 K for w) to the data sets with an Arrhenius-type temperature dependence. Error bars are standard errors.

adatom to stick to already advanced parts of a step, protuberances grow faster in the presence of an ES barrier when steps advance. This destabilizing effect alone would cause perturbations of any wavelength to grow. In a thermodynamic picture, as the amplitude of the fluctuation increases, so does the step length, and thus the step free energy. A capillary-induced smoothing follows, either mediated by diffusion of adatoms along step edges, or evaporation of atoms from steps onto terraces, diffusion, and recondensation. Within the framework of a linear stability analysis a critical wavelength naturally emerges from the balance between these effects [4].

The experimentally observed shift of the instability towards larger wavelengths with increasing surface temperature results from an increasing smoothing efficiency. On the other hand, since the step width is of the same order of magnitude as the mean terrace width (Fig. 2), nonlinear effects are likely to intervene in the evolution of the instability, and conclusions from the linear BZ theory are not easily extrapolated. Recent theoretical studies [6,7] of the BZ instability in the nonlinear regime give evidence that the most unstable wavelength of the linear regime, λ_u , is preserved during subsequent nonlinear evolution of the step profile. These studies consider a smoothing process through evaporation/condensation. Although the extension of these results to the case where smoothing proceeds by step edge diffusion appears to be nontrivial, they tend to favor the interpretation that the wavelength selected by the BZ instability would still be the most unstable one of the linear regime. However, in the following, we show that the selected wavelength observed in our experiment may not have its origin in the standard BZ mechanism.

Within the linear stability analysis [4], the wavelength is extracted from the dispersion relation, defining the relative speeds of growth or decay of all Fourier modes in the perturbation of a straight step. For vicinal Cu surfaces in the temperature range covered by our experiment, capillary-induced smoothing through diffusion along step edges is operative [11]. In this case, the chemical potential gradient along a curved step [5] generates a current involving the diffusion coefficient D_m along a kinked step [11,12]. We have adapted the dispersion relation of BZ to this situation (assuming that desorption of atoms into the gas phase is negligible). Attachment of adatoms to steps is supposed to be instantaneous at ascending steps. By contrast, attachment to descending steps is represented by a kinetic coefficient ν_s , linked to the probability for an adatom to overcome the ES barrier [4]. A characteristic length d_s is defined as $d_s = D_t/\nu_s$, where D_t is the diffusion coefficient on terraces. Focusing on our experimental observations, we consider an in-phase step train. Then, in the long wavelength limit ($\lambda \gg l$), the most unstable mode is given by

$$\lambda_u = 4\pi \left[\frac{\Omega^2 \tilde{\gamma} c_m^{\text{eq}} D_m}{k_B T f_s F l^2} \right]^{1/2}, \quad (1)$$

where $f_s \equiv (d_s/l)/(1 + d_s/l)$, F is the incident flux in ML/s, Ω the atomic area, $\tilde{\gamma}$ the step edge stiffness, c_m^{eq} the equilibrium adatom concentration at the step edge, and k_B the Boltzmann constant.

In order to check the relevance of (1) to our experimental findings, we have to evaluate the order of magnitude and the temperature dependence of the different terms. A good approximation for the step edge stiffness within our temperature range is [13] $\tilde{\gamma} = (k_B T/2a) \exp(E_k/k_B T)$, where E_k is the kink energy. At equilibrium, a simple nearest-neighbor model brings [11] $c_m^{\text{eq}} = (1/a) \exp(-2E_k/k_B T)$. For $d_s \gg l$, one has $f_s \sim 1$ with a weak temperature dependence, and thus a weak contribution to λ_u . We assume that D_m , the diffusion coefficient over a kinked step, can be put in the simple form $D_m = D_m^0 \exp(-E_m/k_B T)$. E_m is the activation energy of the rate limiting process in edge diffusion, i.e., the emission of an adatom from a kink [11].

We find a slope of 76 ± 11 meV for λ (Fig. 2). With relation (1) we identify this energy as $(E_m + E_k)/2$. Noting that f_s decreases with increasing temperature, we then have an upper limit $E_m + E_k \leq 0.15 \pm 0.02$ eV. A slightly higher value is extracted if the deviation from the long wavelength limit is accounted for. As a matter of fact, the experimental slope is intermediate between the ones expected for the long and small wavelength limits, respectively. The condition is then $E_m + E_k \leq 0.23 \pm 0.03$ eV [14]. Given a kink energy $E_k \approx 0.13$ eV [11], we are left with $E_m \leq 0.10 \pm 0.03$ eV, a value much smaller than the experimental result $E_m \approx 0.65$ eV [11,15]. Moreover, beside the very small activation energy E_m , an unphysically small preexponential factor $D_m^0 \sim 10^{-11 \pm 2}$ cm²/s would be required to fit the experimental data. The discrepancy in wavelength between experiment and the linear BZ type mechanism is significant: At 280 K, for example, we observe $\lambda = 85$ Å, while Eq. (1) gives only $\lambda = 5$ Å (11 Å without the long wavelength approximation). We thus infer that the observed selected wavelength is not the most unstable one of the linear BZ regime. As mentioned above, current theories assess that it survives the nonlinear evolution of the system. This leads to the conclusion that the observed growth patterns could possibly also be generated by other mechanisms.

We suggest that the wavelength is imposed through nucleation and island formation at step edges. At that stage, a 1D nucleation length can be defined as [16] $L_n = (12a^3 D_s / F l)^{1/4}$, where D_s is the diffusion coefficient along a straight $\langle 110 \rangle$ step edge. L_n then sets the length scale of the protuberances on the step, which subsequently develop into the observed patterns during step flow in the presence of the ES barrier. The experimentally determined wavelengths are compatible with this process: Assuming $D_s = D_s^0 \exp(-E_s/k_B T)$, we find $E_s = 0.30 \pm 0.04$ eV from the slope in Fig. 2, in fair agreement with another experimental result, $E_s \approx 0.45$ eV [11,15], and $D_s^0 \sim 10^{-6 \pm 2}$ cm²/s. Since the nucleation length equals roughly the size of the compact 1D islands,

smaller protrusions generated by the BZ type mechanism cannot develop, whereas those for which $\lambda \geq L_n$ can. Therefore, we expect this mechanism to supersede the standard BZ scenario, whenever the nucleation length is larger than the critical BZ length. In fact, the nucleation length seems to be the relevant length scale at a given temperature. During two step flow sequences, first at low temperature and subsequently at higher temperature, the system adapts to the high temperature patterns. Reversing the order of sequences results in a crossover to the low temperature morphology.

The presence of a kink ES barrier would, of course, enforce the formation of the characteristic fingers during the evolution of the system. Recently, Pierre-Louis *et al.* [17] and Ramana Murty *et al.* [18] demonstrated that, in fact, an instability generated through an up-kink current induced by a kink ES barrier supersedes the BZ instability for certain step orientations. So far there is no experimental evidence [11] for a kink ES barrier in the class of vicinal Cu surfaces under investigation. Nevertheless, numerical estimates with reasonable assumptions for energetic parameters valid for our system indicate that the meander wavelength would be even smaller as compared to the BZ case, if smoothing proceeds by step edge diffusion. For example, a kink ES barrier as small as 0.02 eV results in a wavelength of $\lambda = 1 \text{ \AA}$ at 280 K. On the other hand, if one takes smoothing due to the stochastic nature of nucleation into account [16], the selected wavelength would be much larger [17] than the nucleation length, for very small kink ES barriers. In this case, step flow could be regarded as being basically stable, so that this mechanism can be discarded. If, however, the kink ES barrier is strong (same order of magnitude as the kink energy), the wavelength is in fact determined by nucleation and island formation [16], just as in 2D systems, where pyramidlike structures develop due to the ES step edge barrier, whose mean separation is set by island formation [2].

In the whole temperature range covered by our experiment, we always observe a specific slope selection along the $\langle 100 \rangle$ direction for the sides of the fingers. Theoretical work [19] demonstrates that the ES barrier shows a strong anisotropy, and may vanish at $\langle 100 \rangle$ oriented steps in fcc lattices, presumably because they provide a maximum density of kinks and therefore an easy pathway for descent. By symmetry, a possible kink ES barrier-induced current should also vanish at this orientation. Thus, when the slope reaches this orientation, the driving force(s) of the instability disappear(s) and growth keeps going in a stationary manner.

In conclusion, homoepitaxial step flow growth on Cu (1,1,17) leads to a lateral patterning of the surface with specific wavelength and slope selections. The latter is likely caused by a pronounced anisotropy of the ES barrier in

this system. The deposition temperature-dependent wavelength is imposed by nucleation and 1D island formation at step edges. This mechanism for wavelength selection should hold whenever the nucleation length is larger than the length scale set by the critical BZ wavelength. This condition should apply for many other systems as well.

Our results raise as well some fundamental open questions. Specifically, does the kink ES barrier exist in these metallic systems? An investigation of the temporal evolution of the slope towards its steady state value would presumably allow us to identify a possible contribution of the kink ES barrier in the development of the observed growth patterns.

We thank P. Lavie and F. Merlet for precious technical support, and T. Einstein for making Ref. [17] available prior to publication.

-
- [1] See, for example, MRS Bull. **23**, 15 (1998).
 - [2] J.-K. Zuo and J.F. Wendelken, Phys. Rev. Lett. **78**, 2791 (1997); H.-J. Ernst *et al.*, *ibid.* **72**, 112 (1994); L.C. Jorritsma *et al.*, *ibid.* **78**, 911 (1997); J.A. Stroscio *et al.*, *ibid.* **75**, 4246 (1995); J.E. Van Nostrand *et al.*, *ibid.* **74**, 1127 (1995).
 - [3] R.L. Schwoebel, J. Appl. Phys. **40**, 614 (1969).
 - [4] G.S. Bales and A. Zangwill, Phys. Rev. B **41**, 5500 (1990).
 - [5] O. Pierre-Louis and C. Misbah, Phys. Rev. B **58**, 2259 (1998); **58**, 2276 (1998); T. Ihle, C. Misbah, and O. Pierre-Louis, *ibid.* **58**, 2289 (1998).
 - [6] O. Pierre-Louis *et al.*, Phys. Rev. Lett. **80**, 4221 (1998).
 - [7] M. Rost, P. Smilauer, and J. Krug, Surf. Sci. **369**, 393 (1996).
 - [8] L. Schwenger, R.L. Folkerts, and H.-J. Ernst, Phys. Rev. B **55**, R7406 (1997).
 - [9] P. Tejedor *et al.*, Surf. Sci. **407**, 82 (1998); Phys. Rev. B **59**, 2341 (1999).
 - [10] At room temperature, step edges appear "frizzed," characteristic of active mass transport along step edges; see Refs. [11,15].
 - [11] M. Giesen-Seibert *et al.*, Phys. Rev. Lett. **71**, 3521 (1993); **73**, E911 (1994); Surf. Sci. **329**, 47 (1995).
 - [12] K. Mussawisade, T. Wichmann, and K. W. Kehr, Surf. Sci. **412/413**, 55 (1998).
 - [13] N. C. Bartelt, T. L. Einstein, and E. D. Williams, Surf. Sci. Lett. **240**, L591 (1990).
 - [14] The slope in the small wavelength limit is $(E_m + E_k)/3$.
 - [15] J. C. Girard *et al.*, Surf. Sci. **301**, 245 (1994).
 - [16] P. Politi and J. Villain, Phys. Rev. B **54**, 5114 (1996); P. Politi, J. Phys. I (France) **7**, 797 (1997).
 - [17] O. Pierre-Louis, M. R. d'Orsogna, and T. L. Einstein, Phys. Rev. Lett. **82**, 3661 (1999).
 - [18] M. V. Ramana Murty and B. H. Cooper, Phys. Rev. Lett. **83**, 352 (1999).
 - [19] U. Kürpick and T. S. Rahman, Phys. Rev. B **57**, 2482 (1998).